Three discontinuity-induced bifurcations to destroy self-sustained oscillations in a superconducting resonator

Mike R. Jeffrey[1]

Abstract

The nonsmooth dynamical model of a superconducting resonator is discussed, based on previous experimental and analytical studies. The device is a superconducting sensor whose key elements are a sensor probe attached to a conducting ring, around which flows an electric current. The ring is interrupted by a microbridge of superconducting material, whose temperature can be altered to sensitively control the device's conductivity. In certain conditions, novel self-sustaining power oscillations are observed, and can suddenly disappear. It was previously shown that this disappearance can be described by a periodic attractor undergoing a catastrophic sliding bifurcation. Here we reveal the sequence of bifurcations that leads up to this event, beginning with the change in stability of a fixed point that creates an attractor, and the birth of a saddle-type periodic orbit by means of a Hopf-like discontinuity-induced bifurcation.

1. Introduction

Sliding is a discontinuity-induced phenomenon that arises in systems of ordinary equations that are piecewise-smooth, meaning the equations are smooth everywhere except on certain hypersurfaces, called *switching manifolds*, where they are discontinuous. A solution is said to *slide* when it evolves along a switching manifold. In mechanics this describes sticking caused by dry friction, in switched control it describes modes confined to codimension one control surfaces, among numerous other engineering and biological applications, see e.g. [3, 5]. In this paper we study the piecewise smooth model of a superconducting resonator, derived in [1, 11, 12, 13] to explain the appearance of novel self-sustaining oscillations, to show how an attractor is created, and the oscillations destroyed, via a sequence of discontinuity-induced bifurcations whose theory that are novel from both theoretical and experimental perspectives.

In the main part of the paper, Secs. 2 to 4, we elaborate on and extend the study of the superconducting resonator, focusing on fixed points and bifurcations of the piecewise-smooth dynamical system rather than the physics of the device, though in the closing remarks, Sec. 4, we revisit this and discuss the model's practical significance. We find three discontinuity-induced bifurcations that occur in sequence, from the creation of a periodic orbit of saddle-type (one positive and one negative eigenvalue), to

---

[1]Department of Engineering Mathematics, University of Bristol, Bristol BS8 1TR, United Kingdom.

its subsequent role in the catastrophic sliding bifurcation that destroys a self-sustaining thermal oscillation. The sequence of bifurcations is confirmed numerically in the limit of fast heat transfer $\epsilon \to 0$, where the system becomes piecewise-linear. The persistence of these results for nonzero ϵ, and their significance in the physical device, are proposed as the subject of further study.

We begin with a brief introduction to piecewise-smooth systems and discontinuity-induced bifurcations. Consider the system

$$\dot{x} = f(x) = \begin{cases} f_+(x) & \text{if} \quad h(x) > 0, \\ f_-(x) & \text{if} \quad h(x) < 0, \end{cases} \qquad (1)$$

where $f_\pm(x) \in \mathbb{R}^n$ and $h(x) \in \mathbb{R}$ are smooth functions of the state $x \in \mathbb{R}^n$, and the dot denotes derivative with respect to time. The condition $h(x) = 0$ implicitly defines a switching manifold which we label Σ.
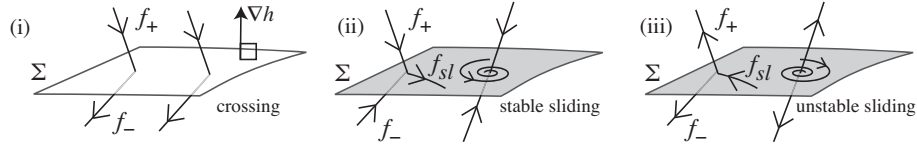

Figure 1: Dynamics at a switching manifold Σ: (i) crossing; (ii) stable sliding, where orbits converge onto the manifold; (iii) unstable sliding, where orbits diverge from the manifold, each in finite time. The system consists of a piecewise-smooth vector field which is discontinuous along Σ (jumps between the values f^+ and f^-), and in (ii)-(iii) this induces a sliding vector field f^{sl} on Σ. Pseudoequilibria – fixed points of the sliding dynamics shown in (ii)-(iii) – are points where f^+ and f^- are antiparallel.

The piecewise-smooth system $dx/dt = f(x)$ can be solved as a differential inclusion, also called a Filippov system [7]. If the vector field points through Σ, meaning $(\nabla h \cdot f_+)(\nabla h \cdot f_-) > 0$, then solutions cross through it as shown in Fig. 1(i). If the vector field points towards or away from Σ on both sides, meaning $(\nabla h \cdot f_+)(\nabla h \cdot f_-) < 0$, we take a convex combination of f_+ and f_-,

$$f_{sl} = \lambda f_+ + (1 - \lambda) f_- \quad \text{where} \quad \lambda = \frac{\nabla h \cdot f_-}{\nabla h \cdot (f_- - f_+)}, \qquad (2)$$

called the *sliding vector field*, with λ defined such that f_{sl} lies in the tangent space of Σ. Sliding orbits are solutions of $\dot{x} = f_{sl}$ on Σ where $\lambda \in (0, 1)$, as illustrated in Fig. 1(ii)-(iii). The following standard distinction between fixed points of $f_\pm$ and f_{sl} is useful:

Definition. *We call a point where $f_+ = 0$ or $f_- = 0$ an* equilibrium, *and a point where $f_{sl} = 0$ a* pseudoequilibrium.

Switching manifolds can cause qualitative changes in a system's dynamics, termed *discontinuity-induced bifurcations* [3]. They include local bifurcations caused when an equilibrium meets a switching manifold, called a *boundary equilibrium bifurcation*. They also include global bifurcations caused when an attracting periodic orbit meets a switching manifold and thereby loses/gains a segment of sliding, called a *sliding bifurcation*. Recently, a topological classification of sliding bifurcations revealed a

2

new class of *catastrophic sliding bifurcations* [9]. In these, instead of losing/gaining a sliding segment, an attracting periodic orbit is destroyed catastrophically, without any significant change in its amplitude or period prior to the bifurcation. (All of these are more thoroughly reviewed in the article *Bifurcations of piecewise smooth flows: perspectives, methodologies and open problems* by A. Colombo et al, also in this journal issue.)

The simplest examples of these three classes of discontinuity-induced bifurcation are illustrated in Fig. 2: (i) a boundary equilibrium bifurcation, (ii) a sliding bifurcation, and (iii) a catastrophic sliding bifurcation, each described in the figure. In this paper we will study an application that involves a sequence of three bifurcations, one in each class, and the particular examples involved are sketched and described in Fig. 3. The boundary equilibrium bifurcation shown involves a change of stability as an equilibrium becomes a pseudoequilibrium, and is therefore reminiscent of the well-known Hopf bifurcation [10], or of the Hopf-like bifurcation in a planar Filippov system derived in [4].
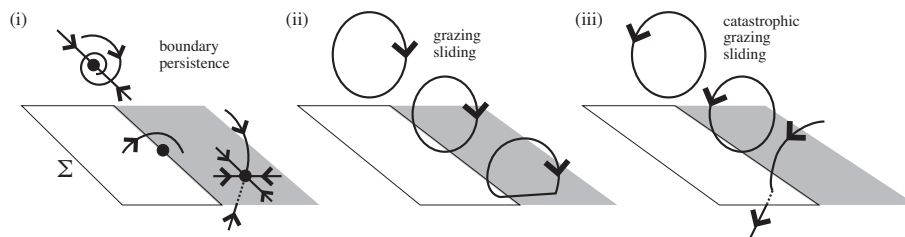

Figure 2: Three examples of discontinuity-induced bifurcations. The switching manifold Σ is made up of sliding regions (shaded) and crossing regions (unshaded), and the bifurcations take place on the boundary between them. Each picture shows three images of a phase portrait changing as a parameter varies: (i) an equilibrium persists when it hits Σ and becomes a pseudoequilibrium; (ii) a periodic attractor persists when it hits Σ and gains a sliding segment; (iii) a periodic attractor is destroyed when it hits Σ. In (i)-(ii) the sliding region is stable and in (iii) it is unstable.
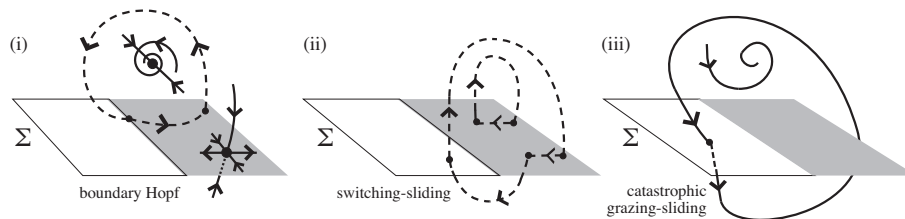

Figure 3: Three discontinuity-induced bifurcations involving unstable sliding. Each picture shows two images of a phase portrait changing as a parameter varies: (i) a stable focus changes stability as it hits Σ, becoming a pseudoequilibrium of saddle-type in an unstable sliding region, and a periodic orbit (also of saddle-type) is annihilated in the process; (ii) a periodic orbit with a sliding segment develops an arc below Σ, by what is called a *switching-sliding* bifurcation in [3]; (iii) a periodic orbit is destroyed by a catastrophic grazing-sliding bifurcation (see [9]).

The theory of discontinuity-induced bifurcations in higher dimensions faces many fundamental difficulties. There are many possible classes of system that can be stud-

3

ied, primarily because switching manifolds come in various forms. Models derived from applications frequently have nontrivial switching manifold topologies, may involve strong simplifications that make the models highly non-generic, and may provide simulated or experimental data of great complexity. Here we study a recent experimentally motivated model, proposed to describe novel self-sustaining thermal oscillations observed in a superconducting resonator device (see [1] and references therein). The model contains many elements that are attractive for a geometrical study. Firstly, it is three dimensional (therefore non-planar, but sufficiently low dimensional to be tractable). Secondly, it contains not only switching behaviour (between normal and super conducting temperature regimes), but also involves singular perturbation, in the form of fast evolution towards surfaces inhabited by slow linear dynamics, and the slow surfaces intersect the switching manifold. In addition, the model is accompanied by clear experimental data that shows destruction of the self-sustaining oscillations, through what was shown in [8] to be a catastrophic sliding bifurcation. The central interesting feature of the superconducting resonator model is that it involves sliding, but contrary to many well studied systems, the sliding dynamics important to the resonator is *unstable*.

At an unstable sliding region (Fig. 1(iii)), orbits everywhere diverge from the switching manifold. The state of a system cannot evolve onto an unstable sliding region in forward time, except at its boundary. The interaction of attractors with the boundary of unstable sliding is central to the existence of catastrophic sliding bifurcations [9].

2. Piecewise-smooth model of a superconducting resonator

The superconducting resonator is an experimental device, designed as a sensor whose fine sensitivity could be controlled by laser heating of a niobium nitride (NbN) microbridge [13]. The microbridge sits around the circumference of a conducting ring attached to a sensor probe. In experiment, however, novel self-sustaining oscillations are observed [1, 11, 12, 13]. They have a simple physical origin, namely the oscillation of the microbridge between normal and superconducting states: at a low temperature the microbridge is superconducting, passing a high current which heats the bridge, until its temperature exceeds the threshold where it ceases to be superconducting, the conductance falls, the current therefore decreases and the heating effect drops, so the bridge temperature falls below the threshold, the bridge becomes superconducting, and the process is seen to repeat periodically. The result is that periodic oscillations are observed in the device's power output for certain experimental parameters. It was observed, however, that these self-sustaining oscillations could vanish suddenly, without significant prior change in period or amplitude, after which the system would settle to a stable fixed point in either the normal or superconducting temperature range.

The non-dimensionalized dynamical model proposed for the device [1, 8] can be expressed in terms of the power in the ring, whose complex amplitude is given by β, and the temperature θ of the microbridge, satisfying

$$\begin{aligned}
\dot{\beta} &= \Lambda(\theta)\beta - i, \\
\epsilon\dot{\theta} &= s(\theta)|\beta|^2 - \theta,
\end{aligned} \tag{3}$$

where $i = \sqrt{-1}$. The positive constant ϵ is small, indicating that heat transfer from the microbridge to a surrounding coolant is very fast compared to the dynamics of the power amplitude β. The parameters $s \in \mathbb{R}$ and $\Lambda \in \mathbb{C}$ relate the response of the ring respectively to the driving amplitude and frequency. Their temperature dependence can be expressed as piecewise-smooth constant, jumping at a switching manifold Σ given by $\theta = 1$, between normal ($\theta > 1$) and super ($\theta < 1$) conducting modes. Denoting the modes by $+$ and $-$, we let

$$\Lambda(\theta) = \begin{cases} \Lambda_+ & \text{if } \theta > 1, \\ \Lambda_- & \text{if } \theta < 1, \end{cases} \quad \text{and} \quad s(\theta) = \begin{cases} s_+ & \text{if } \theta > 1, \\ s_- & \text{if } \theta < 1. \end{cases} \quad (4)$$

Physical values of the constants $\Lambda_\pm$ and $s_\pm$ lie in the ranges $\mathrm{Re}\, \Lambda_\pm < 0$ and $s_+ > s_- > 0$ [8].

Three surfaces are illustrated in Fig. 4(i) that play a vital role in the dynamics. These include the θ-nullclines of (3), which are

$$\begin{aligned} \Sigma_+ &= \{(\beta, \theta) : \eta_+(\beta, \theta) = 0, \theta > 1\}, \\ \Sigma_- &= \{(\beta, \theta) : \eta_-(\beta, \theta) = 0, \theta < 1\}, \end{aligned} \quad (5)$$

where

$$\eta_\pm(\beta, \theta) = s_\pm |\beta|^2 - \theta. \quad (6)$$

(Treated as a singular perturbation problem, $\Sigma_\pm$ are critical manifolds, however the theory of normally hyperbolic manifolds [6] does not apply near the switching manifold Σ.) For $\epsilon \ll 1$ the system (3) splits into fast dynamics, where the large $\dot\theta$ component pushes the state towards $\Sigma_\pm$, and slow dynamics in a neighbourhood of $\Sigma_\pm$ (where $\dot\theta = 0$), where the system reduces to the linear $\dot\beta$ equation. This is illustrated in Fig. 4(i), with (ii)-(iii) showing different representations that we make use of in Sect. 4.
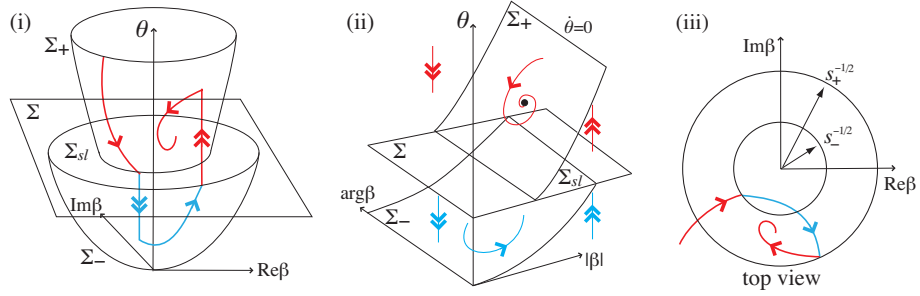

Figure 4: Dynamics of the superconducting resonator. A switching manifold Σ separates normal (above Σ) and super (below Σ) conducting modes. Orbits flow fast (double arrows) towards the slow (single arrows) critical manifolds $\Sigma_\pm$, and away from the unstable sliding region Σ_{sl}. Three projections are shown: (i) in coordinates $(\mathrm{Re}\beta, \mathrm{Im}\beta, \theta)$, (ii) in coordinates $(|\beta|, \arg \beta, \theta)$, (iii) a top view into the complex β plane.

The third important surface is the region on Σ delimited by its intersection with $\Sigma_\pm$, giving the annular region in Figs. 4 (i) & (iii) and the strip in (ii), defined as

$$\Sigma_{sl} = \left\{(\beta, \theta) : \theta = 1, |\beta|^2 \in (1/s_-, 1/s_+)\right\}. \quad (7)$$

5

Σ_{sl} is a region of unstable sliding, where the vector fields in (3) point away from Σ (recall Fig. 1(iii)). The sliding vector field, by (2), is given by

$$\dot{\beta} = \frac{\Lambda_+ \eta_-(\beta, 1) - \Lambda_- \eta_+(\beta, 1)}{\eta_-(\beta, 1) - \eta_+(\beta, 1)} \beta - \mathrm{i} \quad \text{on} \quad \Sigma_{sl}. \tag{8}$$

Elsewhere the flow crosses Σ. The three regions Σ_{sl}, Σ_+, and Σ_-, form a continuous (but nonsmooth) surface upon which $\dot{\theta} = 0$.

3. Equilibria and pseudoequilibria in the model

Given that $\dot{\theta}$ vanishes only on Σ_{sl} or $\Sigma_\pm$, we know that any fixed points of the piecewise-smooth system must be contained within these surfaces, in the form of equilibria where (3) vanishes, and pseudoequilibria where (8) vanishes.

Lemma 1. *(i) A stable focus exists on Σ_+ if and only if $\eta_+(\mathrm{i}/\Lambda_+, 1) > 0$.*
(ii) A stable focus exists on Σ_- if and only if $\eta_-(\mathrm{i}/\Lambda_-, 1) < 0$.

Proof. The system (3)-(4) has zeros at $(\beta, \theta) = (\beta_\pm^{eq}, \theta_\pm^{eq}) \equiv (\mathrm{i}/\Lambda_\pm, s_\pm/|\Lambda_\pm|^2)$. Each solution $(\beta_\pm^{eq}, \theta_\pm^{eq})$ is only valid if it lies on its respective surface $\Sigma_\pm$, that is: (i) if $\theta_+^{eq} > 1$, implying $\eta_+(\mathrm{i}/\Lambda_+, 1) > 0$, and (ii) if $\theta_-^{eq} < 1$, implying $\eta_-(\mathrm{i}/\Lambda_-, 1) < 0$. Both of these are stable foci, because the Jacobian matrix of (3) at $(\beta_\pm^{eq}, \theta_\pm^{eq})$ has one negative eigenvalue $-1/\epsilon$, and two complex eigenvalues with negative real parts $\mathrm{Re}\Lambda_\pm < 0$. $\square$

The only other fixed points in this system are the pseudoequilibria on Σ_{sl}, where (8) vanishes. For these we have:

Lemma 2. *The number of pseudoequilibria, where (8) vanishes, is:*

$$1 \quad \text{if} \quad \eta_+(\Lambda_+, 1)\eta_-(\Lambda_-, 1) < 0, \tag{9}$$

$$0 \quad \text{if} \quad \eta_+(\Lambda_+, 1)\eta_-(\Lambda_-, 1) > j^2/|\Lambda_+\Lambda_-|^2 > 0, \tag{10}$$

$$0 \quad \text{if} \quad \eta_+(\Lambda_+, 1)\eta_-(\Lambda_-, 1) > 0, \quad \text{and} \quad j/|\Lambda_-|^2\eta_-(\Lambda_-, 1) > 0, \tag{11}$$

$$2 \quad \text{if} \quad \frac{j^2}{|\Lambda_+\Lambda_-|^2} > \eta_+(\Lambda_+, 1)\eta_-(\Lambda_-, 1) > 0 \quad \text{and} \quad \frac{j}{|\Lambda_-|^2\eta_-(\Lambda_-, 1)} < 0, \tag{12}$$

where $j = \frac{1}{2}(s_- + s_+) - \mathrm{Re}\left[\Lambda_+\Lambda_-^\star\right]$.

Proof. Instead of solving for the zeros of (8), it is easier to note from (2) (and as illustrated in Fig. 1), that a pseudoequilibrium occurs at a point on Σ_{sl} when there exists $\mu < 0$, such that the upper $(+)$ and lower $(-)$ vector fields in (3)-(4) satisfy

$$\begin{aligned} \Lambda_+\beta - \mathrm{i} &= \mu(\Lambda_-\beta - \mathrm{i}), \\ s_+|\beta|^2 - 1 &= \mu(s_-|\beta|^2 - 1). \end{aligned} \tag{13}$$

Eliminating β from (13) we find

$$\mu = \frac{j \pm \sqrt{j^2 - |\Lambda_+\Lambda_-|^2\eta_+(\mathrm{i}/\Lambda_+, 1)\eta_-(\mathrm{i}/\Lambda_-, 1)}}{|\Lambda_-|^2\eta_-(\mathrm{i}/\Lambda_-, 1)}. \tag{14}$$

Real negative values of μ therefore occur as listed in (9)-(12), and each real positive solution corresponds to a zero of the unstable sliding vector field. $\square$

Lemma 3. *The number of fixed points in the resonator system is either 1 or 3.*

Proof. Combining Lemmas 1 and 2 we have the following cases: if $\eta_+(\Lambda_+, 1) > 0 > \eta_-(\Lambda_-, 1)$ there exists one pseudoequilibrium on Σ_{sl} and one equilibrium on each of Σ_+ and Σ_-; if $\eta_+(\Lambda_+, 1) < 0 < \eta_-(\Lambda_-, 1)$ there exists one pseudoequilibrium on Σ_{sl} but there are no equilibria on Σ_- or Σ_+; if $\eta_+(\Lambda_+, 1)\eta_-(\Lambda_-, 1) < 0$ there are either 2 or 0 pseudoequilibria on Σ_{sl}, and one equilibrium either on Σ_+ or Σ_- but not both. In each case the total number of equilibria and pseudoequilibria is 1 or 3. $\square$

Lemma 3 permits the number of fixed points to change as the parameters $\Lambda_\pm$ or $s_\pm$ are varied. Since these fixed points must lie on Σ_{sl} or $\Sigma_\pm$, they can appear/disappear in only two ways, given by the following two lemmas.

Lemma 4. *Pseudoequilibria undergo a saddle-node bifurcation when both μ values in (14) coincide.*

This can be proven from (8). For brevity we remark only that it is implied by Lemma 2: when $j^2 = |\Lambda_+\Lambda_-|^2\eta_+(\Lambda_+, 1)\eta_-(\Lambda_-, 1)$, two pseudoequilibria coincide and under perturbation there exist either 0 or 2, and since the sliding vector field is smooth on Σ, this constitutes a saddle-node bifurcation.

Lemma 5. *Equilibria pass continuously between Σ_{sl} and either Σ_+ or Σ_-, respectively when $\eta_+(i/\Lambda_+, 1) = 0$ or $\eta_-(i/\Lambda_-, 1) = 0$.*

Proof. By Lemmas 1-2, when $\eta_+(i/\Lambda_+, 1)\eta_-(i/\Lambda_-, 1) < 0$ and $\eta_+(i/\Lambda_+, 1) < 0$, the only fixed point in the system is a pseudoequilibrium on Σ_{sl}. If $\eta_+(i/\Lambda_+, 1)$ changes sign with $\eta_-(i/\Lambda_-, 1) \neq 0$, an equilibrium appears on Σ_+, and simultaneously the pseudoequilibrium vanishes because $\eta_+(i/\Lambda_+, 1)\eta_-(i/\Lambda_-, 1)$ changes sign. To state that a fixed point has passed from Σ_{sl} to Σ_+, it remains to show that it disappeared from Σ_{sl} and appeared in Σ_+ at the same coordinates. The transition takes place when $\eta_+(i/\Lambda_+, 1) = 0$, which means the equilibrium on Σ_+ lies on the intersection of Σ_+ with Σ_{sl}, therefore $\eta_+(\beta, 1) = 0$ and $\beta = i/\Lambda_+$. From (8), the sliding vector field at that point is zero, hence the zeros of Σ_{sl} and Σ_+ coincide there. The argument for fixed points passing from Σ_{sl} to Σ_- when $\eta_-(i/\Lambda_-, 1) = 0$ is analogous. $\square$

Lemma 5 describes a boundary equilibrium bifurcation. However, the fixed point's stability must change when it passes from Σ_{sl} to $\Sigma_\pm$, because a focus on $\Sigma_\pm$ is stable by Lemma 1, while a pseudoequilibrium on Σ_{sl} is repelling at least in the direction normal to Σ_{sl}. Generically, in a smooth dynamical system, when an equilibrium changes stability as one parameter changes, it does so via a Hopf bifurcation: two eigenvalues of the equilibrium cross the imaginary axis, and a limit cycle is created or destroyed. Although Hopf-like boundary equilibrium bifurcations have been studied in planar Filippov systems, see [4], such results have not yet been extended to higher dimensions.

In the following section we will give numerical verification of the following:

Conjecture 6. *When a fixed point moves from Σ_{sl} to Σ_+ or Σ_-, a periodic orbit of saddle-type is created; this boundary equilibrium bifurcation therefore corresponds qualitatively to a subcritical Hopf bifurcation.*

The root of this conjecture lies in the limit of small ϵ (though note that so far we have made no assumptions on the size of ϵ in Lemmas 1-5). Let $\epsilon = 0$ in (3), then in

$\theta > 1$ orbits converge infinitely fast towards Σ_+, in $\theta < 1$ they converge infinitely fast towards Σ_-, thus $\Sigma_\pm$ become switching manifolds upon which stable sliding occurs.

Let us say that a Hopf-like bifurcation occurs if the transition of a fixed point from Σ_{sl} to $\Sigma_\pm$ involves two of its eigenvalues crossing the imaginary axis (not necessarily in a continuous fashion), accompanied by the creation of a limit cycle in the neighbourhood of the fixed point. The only way a periodic orbit can exist in the neighbourhood of the fixed point is if it passes through Σ_{sl}, implying that it is unstable in one direction, and also passes through Σ_+ or Σ_- (whichever the fixed point moves to), implying that it is stable in one direction. This implies that the periodic orbit is of saddle type, having one stable (negative) and one unstable (positive) eigenvalue. In the following section we confirm that, indeed, a saddle-type periodic orbit exists when the fixed point is on Σ_+, and that its transition from Σ_{sl} resembles a subcritical Hopf bifurcation.

4. The three bifurcations

Fig. 5 shows the Hopf-like boundary equilibrium bifurcation conjectured at the end of the previous section. The top row of Fig. 5 shows a sketch in the coordinate system depicted in Fig. 4(ii), and the bottom row shows a numerical simulation of (3) with $\epsilon = 0$, using the top view depicted in Fig. 4(iii). The simulations confirm that a Hopf-like boundary equilibrium bifurcation is indeed observed: a saddle pseudoequilibrium on Σ_{sl} becomes a stable focus equilibrium on Σ_+, and develops a saddle-type periodic orbit; this is as introduced in Fig. 3(i)
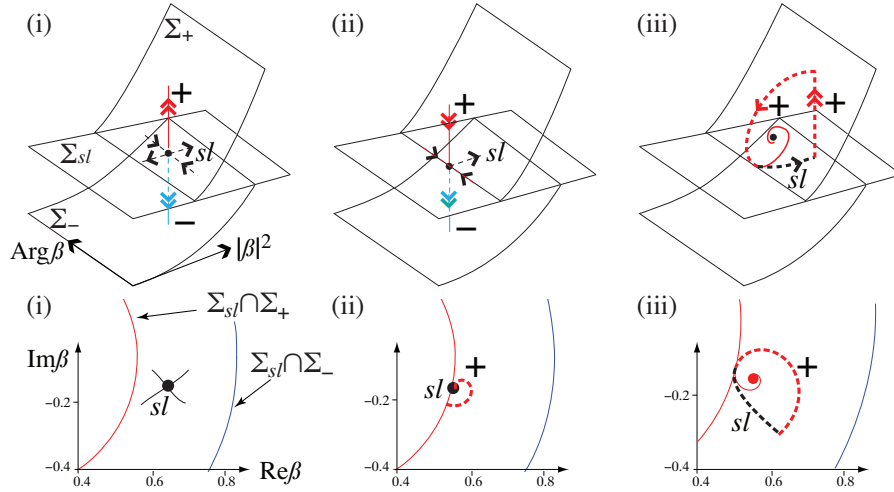

Figure 5: A Hopf-like bifurcation in the resonator model. Top row shows a sketch, and bottom row shows a simulation of (3) with $\epsilon = 0$. In (i) a saddle-type pseudoequilibrium lies on Σ_{sl}. In (ii) the fixed point lies on the boundary between Σ_{sl} and Σ_+. In (iii) the fixed point becomes a stable focus equilibrium on Σ_+, surrounded by a saddle-type periodic orbit (dashed) with a segment on the stable surface Σ_+ and unstable sliding region Σ_{sl}. Orbits are labeled $+, -, sl$, according to whether they lie on Σ_+, Σ_- or Σ_{sl} (coloured respectively red, blue, black, in colour version). Parameters are $s_+ = 3.891$, $s_- = 1.297$, $\Lambda_- = -0.2 + i$, $\mathrm{Re}\Lambda_+ = -0.5$ with: (a) $\mathrm{Im}\Lambda_+ = 2.2$, (b) $\mathrm{Im}\Lambda_+ = 1.9$, (c) $\mathrm{Im}\Lambda_+ = 1.7$.

Now consider what happens as the periodic orbit in Fig. 5 grows, shown in Fig. 6. Eventually it may intersect the boundary between Σ_{sl} and Σ_- as in Fig. 6(ii), and in doing so it can develop a segment on Σ_-, Fig. 6(iii). The transition in (ii) is a switching-sliding bifurcation of a saddle-type periodic orbit, as depicted earlier in Fig. 3(ii).
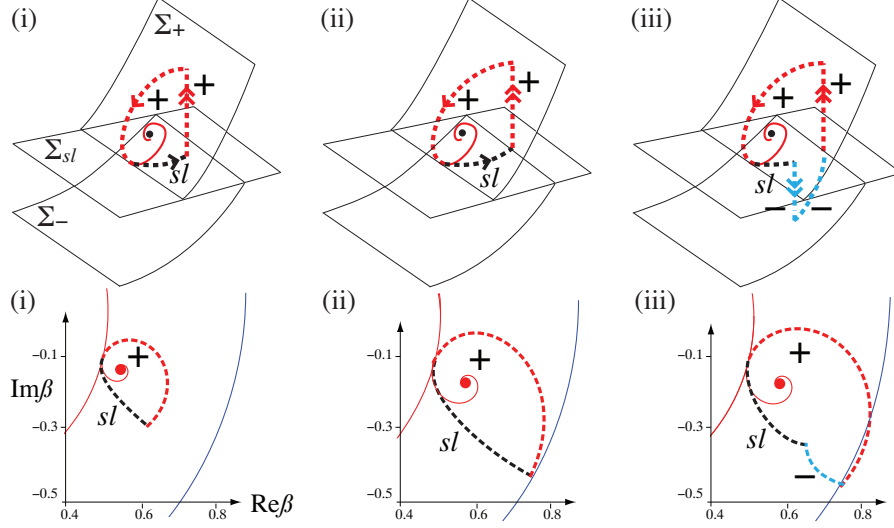

Figure 6: A switching-sliding bifurcation of a piecewise-smooth saddle-type periodic orbit in the resonator model. Top row shows a sketch, and bottom row shows a simulation, continued from Fig. 5. From (i) to (iii) the periodic orbit (dashed) grows and develops a segment that jumps off Σ_{sl} onto Σ_-. Parameter values and labels are as in Fig. 5, with: (a) $\text{Im}\Lambda_+ = 1.6$, (b) $\text{Im}\Lambda_+ = 1.58$, (c) $\text{Im}\Lambda_+ = 1.573$.

A second, stable, periodic orbit exists in the system; it has been omitted from Figs. 5-6 for clarity, but we now shown it in Fig. 7(i). Unlike the saddle-type periodic orbit above, implicit formulae for the stable periodic orbit are known, derived in [8]. Moreover, it is known that the stable periodic orbit suddenly vanishes as a parameter is varied continuously. An explanation for this was provided in [8], with existence conditions, in terms of the catastrophic grazing-sliding bifurcation, similar to Fig. 3(iii). We will now see that the saddle-type periodic orbit, born in Fig. 5 and growing through Fig. 6, is also involved in this bifurcation.

As shown in Fig. 7(i), the saddle periodic orbit now visits all three regions Σ_{sl}, Σ_+, and Σ_-, while the stable periodic orbit visits only the stable regions Σ_+ and Σ_-. The stable orbit shrinks and develops a tangency to the boundary of Σ_{sl} in Fig. 7(ii). Meanwhile the saddle orbit grows until at least part of it coincides with the stable orbit. Interestingly, the two periodic orbits do not fully coincide when the catastrophic sliding bifurcation takes place in Fig. 7(ii) (as they would, for instance, in a saddle-node bifurcation of periodic orbits, see e.g. [10]). Under further parameter variation, Fig. 7(iii), both periodic orbits vanish.
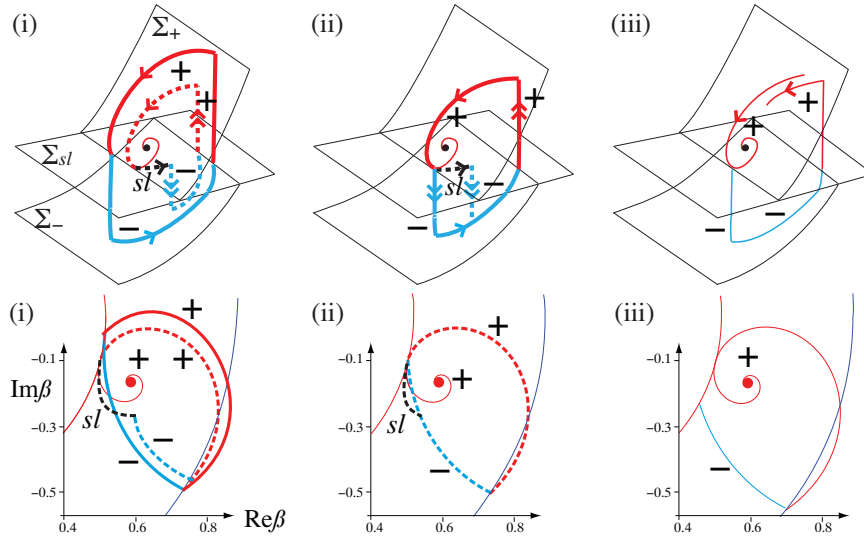
Figure 7: Catastrophic grazing-sliding bifurcation in the superconducting resonator model. Top row shows a sketch and bottom row shows a simulation, continued from Fig. 6. In (i) a stable periodic orbit (bold curve, omitted from Figs. 5-6 for clarity) and the smaller saddle-type periodic orbit (dashed curve). In (ii) the two orbits coalesce by forming a tangency to Σ, at which the forward evolution is nonunique – a solution could follow the periodic orbit or evolve towards the focus. In (iii) all solutions evolve towards a stable focus. Parameters are as in Fig. 5 with: (a) $\mathrm{Im}\Lambda_+ = 1.572$, (b) $\mathrm{Im}\Lambda_+ = 1.57$, (c) $\mathrm{Im}\Lambda_+ = 1.56$.

5. Concluding Remarks

In this paper we have calculated the fixed points of temperature and power dynamics in an experimentally motivated model of a superconducting resonator device. The model involves features of both discontinuity, between normal and super conducting temperature regimes, and singular perturbation, due to a large heat transfer coefficient $1/\epsilon$. Note that Lemmas 1-5 apply to nonzero ϵ, and while we provided numerical evidence supporting Conjecture 6 in the singular limit $\epsilon = 0$ of instantaneous heat transfer, we propose that the Conjecture remains true for nonzero ϵ. One might easily test Conjecture 6 numerically for nonzero ϵ by smoothing out (or 'regularizing') the discontinuity at Σ. However, in the current absence of a theory to say how the choice of such smoothing will affect the system, one cannot be certain how closely it corresponds to the original discontinuous model; further work is needed.

The Hopf-like boundary equilibrium bifurcation found here is of interest because little is known about boundary equilibrium bifurcations in non-planar systems (a notable exception being fold or persistence criteria given in [3]), particularly in the presence of singular perturbation. The periodic orbits are of interest partly because geometric singular perturbation theory could be used to establish whether they persist for nonzero ϵ in a *smooth* system, but little is known in general about the effect of discontinuity and, in particular, of sliding, that are faced in the resonator model. The question therefore remains open as to whether the fixed points, periodic orbits, and bifurcations described here are robust phenomena.

To address the issue of robustness, one could assume that the piecewise-smooth model is an approximation to some smooth system, in which certain regions of state space are squashed, or "pinched", to form switching manifolds. In [2] it was shown that pinching can be used to study nonlinear phenomena such as bifurcations and canards in singularly perturbed systems. First, assume that in coordinates (β, Θ), the resonator's dynamics satisfy the continuous system

$$\begin{array}{rclll} \dot{\beta} & = & \Lambda_+ \beta - \mathrm{i} & + & a(\beta, \Theta), \\ \dot{\epsilon}\Theta & = & s_+ |\beta|^2 - \Theta & + & b(\beta, \Theta), \end{array} \qquad (15)$$

where a and b are continuous and satisfy $a, b \approx 0$ for $\Theta > 1 + \kappa$, and $a \approx (\Lambda_- - \Lambda_+)\beta$, $b \approx (\Lambda_- - \Lambda_+)|\beta|^2$ for $\Theta < 1 - \kappa$, for some small $\kappa > 0$. We then make a nonsmooth coordinate transformation $\theta = \Theta - \kappa \mathrm{sgn}(\Theta - 1)$. When we substitute $\Theta \mapsto \theta$, the zone $|\Theta - 1| < \kappa$ is effectively pinched out of the phase space, and replaced by the switching manifold $\theta = 1$, with the region $1/s_+ < |\beta|^2 < 1/s_-$ forming Σ_{sl}. Then (3)-(4) approximate (15) for $|\Theta - 1| > \kappa$, and the sliding vector field approximates (15) for $|\Theta - 1| < \kappa$ where $|\beta|^2 \in (1/s_+, 1/s_-)$. If we simply choose, for example, $a = b = 0$ for $\Theta > 1 + \kappa$, and $a = (\Lambda_- - \Lambda_+)\beta$, $b = (\Lambda_- - \Lambda_+)|\beta|^2$ for $\Theta < 1 - \kappa$, with a, b, monotonic on $|\Theta - 1| < \kappa$, we obtain what is known as a regularisation of (3), see e.g. [14]. The different forms that a and b may take, and their effect on the dynamics, are not well understood in general.

The superconducting resonator model developed in [1, 11, 12, 13] is intriguing to study from the point of view of the still young bifurcation theory of piecewise-smooth systems. Moreover, it is vital to reliable operation of the physical device that the cause of self-sustaining oscillations is identified, that the parameters for which they and other attractors exist are found. Indeed, these were the motivating factors in deriving the mathematical model, namely to explain novel experimental behaviour. The catastrophic sliding bifurcation in Fig. 7 (and sketched in Fig. 3(iii)) can be clearly seen in experimental time traces from the resonator (see for example [1]), and diagrams showing the stability zones from theory and experiment were produced in [8] and [1] respectively. Nevertheless, a precise quantitative comparison between theory and observations remains a subject for ongoing study.

References

[1] G. Bachar, E. Segev, O. Shtempluck, E. Buks, and S. W. Shaw. Noise induced intermittency in a superconducting microwave resonator. *arXiv:0810.0964*, 2008.

[2] M. Desroches and M. R. Jeffrey. Canard à l'orange: a new recipe for studying relaxation oscillations. *Nonlinearity*, submitted 2010.

[3] M. di Bernardo, C. J. Budd, A. R. Champneys, and P. Kowalczyk. *Piecewise-Smooth Dynamical Systems: Theory and Applications*. Springer, 2008.

[4] M. di Bernardo, A. Nordmark, and G. Olivar. Discontinuity-induced bifurcations of equilibria in piecewise-smooth and impacting dynamical systems. *Physica D*, 237:119–136, 2008.

[5] B. Brogliato, *Nonsmooth mechanics - models, dynamics and control*. Springer-Verlag (New York), 1999.

[6] N. Fenichel, Geometric singular perturbation theory for ordinary differential equations. *J. Differential Equations* **31**(1):53–98, 1979.

[7] A. F Filippov. *Differential Equations with Discontinuous Righthand Sides*. Kluwer Academic Publishers, Dortrecht, 1998.

[8] M. R. Jeffrey, A. R. Champneys, M. di Bernardo, and S. W. Shaw. Catastrophic sliding bifurcations and onset of oscillations in a superconducting resonator. *Phys. Rev. E*, 81(1):016213–22, 2010.

[9] M. R. Jeffrey and S. J. Hogan. The geometry of generic sliding bifurcations. *SIREV*, accepted 2010.

[10] Y. A. Kuznetsov. *Elements of Applied Bifurcation Theory*. Springer, 2nd Ed., 1998.

[11] E. Segev, B. Abdo, O. Shtempluck, and E. Buks. Extreme nonlinear phenomena in NbN superconducting stripline resonators. *Physics Letters A*, 366(1-2):160 – 164, 2007.

[12] E. Segev, B. Abdo, O. Shtempluck, and E. Buks. Novel self-sustained modulation in superconducting stripline resonators. *EPL*, 78(5):57002 (5pp), 2007.

[13] E. Segev, B. Abdo, O. Shtempluck, and E. Buks. Thermal instability and self-sustained modulation in superconducting NbN stripline resonators. *J. Phys: Condens. Matter*, 19(9):096206(14pp), 2007.

[14] M. A. Teixeira, J. Llibre, and P. R. da Silva. Regularization of discontinuous vector fields on $\mathbb{R}^3$ via singular perturbation. *J.Dyn.Diff.Equat.*, 19(2):309–331, 2007.